# An Overlooked yet Ubiquitous Fluoride Congenitor: Binding Bifluoride in Triazolophanes Using Computer-Aided Design

Raghunath O. Ramabhadran,[†] Yun Liu,[†] Yuran Hua, Moira Ciardi, Amar H. Flood,* and Krishnan Raghavachari*

Department of Chemistry, Indiana University, 800 East Kirkwood Avenue, Bloomington, Indiana 47405, United States

**S** *Supporting Information*

**ABSTRACT:** Despite its ubiquity during the binding and sensing of fluoride, the role of bifluoride ($HF_2^-$) and its binding properties are almost always overlooked. Here, we give one of the first examinations of bifluoride recognition in which we use computer-aided design to modify the cavity shape of triazolophanes to better match with $HF_2^-$. Computational investigation indicates that $HF_2^-$ and $Cl^-$ should have similar binding affinities to the parent triazolophane *in the gas phase*. Evaluation of the binding geometries revealed a preference for binding of the linear $HF_2^-$ along the north–south axis with a smaller Boltzmann weighted population aligned east–west and all states being accessed rapidly through in-plane precessional rotations of the anion. While the ^{1}H NMR spectroscopy studies are consistent with the calculated structural aspects, binding affinities *in solution* were determined to be significantly smaller for the bifluoride than the chloride. Computed geometries suggested that a 20° tilting of the bifluoride (stemming from the cavity size) could account for the 25-fold difference between the two binding affinities, $HF_2^- < Cl^-$. Structural variations to the triazolophane's geometry and electronic modifications to the network of hydrogen bond donors were subsequently screened in a stepwise manner using density functional theory calculations to yield a final design that eliminates the tilting. Correspondingly, the bifluoride's binding affinity ($K \sim 10^6\ M^{-1}$) increased and was also found to remain equal to chloride *in the gas and solution phases*. The new oblate cavity appeared to hold the $HF_2^-$ in a single east–west arrangement. Our findings demonstrate the promising ability of computer-aided design to fine-tune the structural and electronic match in anion receptors as a means to control the arrangement and binding strength of a desired guest.
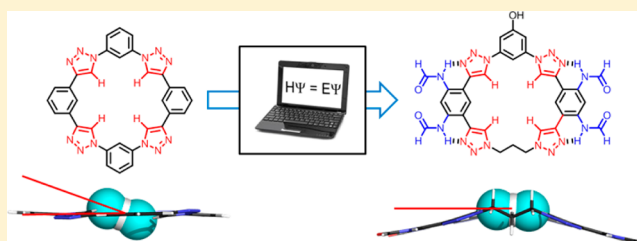
## INTRODUCTION

The importance of anions in chemistry and biology[1] continues to motivate studies of their recognition. For instance, during the remediation of radionuclides ($^{99}TcO_4^-$) and counteranions ($SO_4^{2-}$) present in the nuclear fuel cycle. Triazolophanes[2,3] are among the newest receptors in this area that are characterized by their modularity and use of activated CH hydrogen bonds[4] with a size selectivity for chloride. We are now pushing the limits of the cavity's spherical shape to bind more complex anions, a situation stemming from the fact that polyatomic anions can be pseudospherical under the right circumstances. For instance, we showed that spherical $Cl^-$ and linear diatomic $CN^-$ have equal binding affinities[3b] to tetraphenylene triazolophanes, since the cyanide's in-plane orientation is rotationally averaged. Taking steps towards polyatomic anions led us to consider the binding of bifluoride ($HF_2^-$), the smallest of the linear triatomic anions. This ion also attracted our attention since its internal hydrogen bonds are the strongest[5] known, making it a symbolic antonym of the so-called weak CH hydrogen-bonding systems like triazolophanes.

While little appears to be known about bifluoride, we believe that it may be more prevalent than first thought. Binding studies are rare—two to date[6,7] and two known crystal structures.[6a,8] Bifluoride has seen some use in the preparation of metal complexes[9] for fluorine-related chemical transformations[10] and recently as a synthon in the emerging area of self-assembled networks.[11] Industrially, it is perhaps more widely known where it is used as buffered oxide etch (BOE)[12] for the fabrication of silicon semiconductors, for digestion,[13] extraction,[14] and as a cleaning agent in automatic car washers.[15] A few toxicity studies have also emerged[16] suggesting that it acts like fluoride while showing fewer of the telltale signs of exposure.[17] Thus, during the course of our study, we were surprised to discover that bifluoride is not rare at all. Instead, it is frequently observed in studies of fluoride recognition and sensing due to the fact that bifluoride forms readily[18–22] by abstraction of protons:

$$2F^- + RH \rightleftharpoons HF + R^- + F^- \rightleftharpoons HF_2^- + R^- \qquad (1)$$
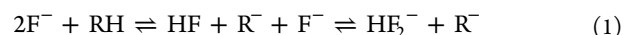
In fact, we found that the only situation when bifluoride is not present in appreciable amounts (>1 mol %), relative to $F^-$, is in aqueous solutions at concentrations less than 10 mM or in basic solutions, i.e., pH >7. Despite bifluoride's prevalence, it is consistently unnoticed or overlooked in the field of anion recognition, though it is almost always capable of serving as a

Scheme 1. Computer-Aided Design on Receptor 1 Leads to the Development of Macrocycle 2[a]
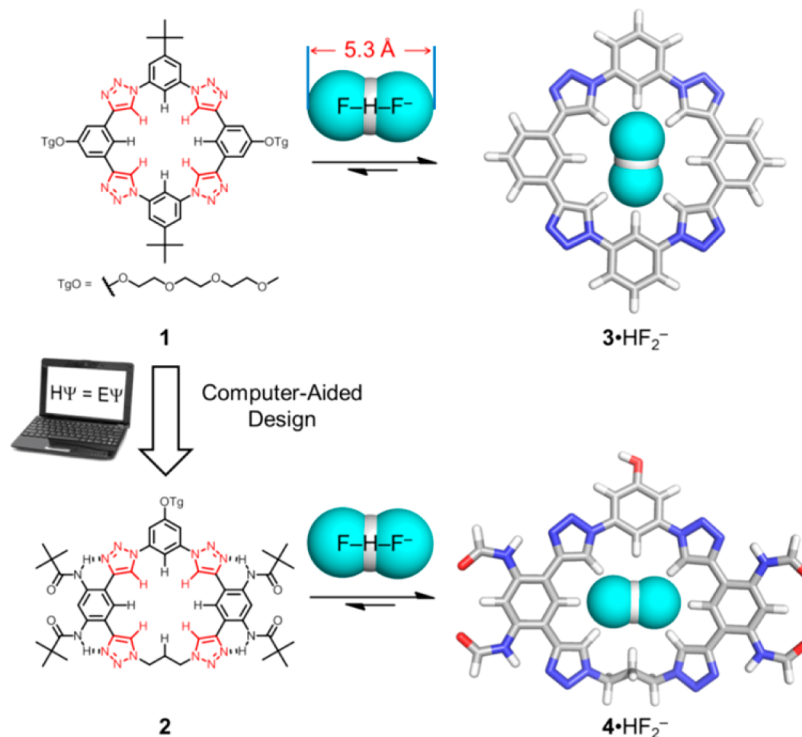


[a]Simplified structures ($3 \cdot HF_2^-$ and $4 \cdot HF_2^-$) were optimized using M06-2X/6-31+G(d,p) and shown to have different preferred bifluoride orientations.

competing interferant in fluoride binding.[23] As noted by Cametti and Rissanen in their review on fluoride binding,[23] we too wonder how many of the hundreds of papers devoted to fluoride recognition in the past 10 years carry a systematic error associated with the bifluoride present. It is clear that careful studies of bifluoride binding are long overdue.

Bowman-James's bicyclic azacryptand,[6] Eichen's cyclic benzoimidazole derivative,[7] and Severin's metallo-macrocycle[8] are the only studies of $HF_2^-$ binding that we are aware of. The first two studies arose by serendipity during fluoride binding. In particular, the elliptical cavity of the bicyclic azacryptand was shown to bind linear anions ($HF_2^-$, $N_3^-$) with greater strength than spherical anions ($Cl^-$, $Br^-$, $I^-$).[6b] Consequently, significant and selective binding toward $HF_2^-$ in dimethyl sulfoxide (DMSO) was achieved. The cyclic benzoimidazole was shown to bind $HF_2^-$ strongly in DMSO ($K \sim 10^5$), yet its $F^-$ binding strength was not determined on account of the formation of $HF_2^-$. Lastly, Severin's metallo-macrocycle was found to bind $HF_2^-$ as a contact ion pair with $Li^+$.[8] Even though $HF_2^-$ was added intentionally to characterize the host–guest complex in the solid state, solution-based titrations were not performed. Thus, a detailed study focusing primarily on the characterization of the binding properties of $HF_2^-$ will be crucial to aid in an improved understanding of this anion's recognition properties and to help deliver better guidance to the role of bifluoride in the active area surrounding the chelating and sensing of fluoride.[24]

In this work, bifluoride was chosen to test the shape selectivity of anion binding to the rigid triazolophane macrocycle. On the basis of the detailed understanding provided by the prior use of coupled experiment-theory studies on triazolophanes,[2f,3,25,26] we decided that a computer-aided-design approach can be fruitfully used to reshape the receptor

to appropriately accommodate $HF_2^-$ with an enhanced binding energy. Such computer-aided-design approaches represent an ideal situation, since virtual experiments can be conducted in lieu of observational ones to quickly advance understanding and to direct the rational design of molecular targets. In the field of anion recognition, Hay and co-workers advocate the use of HostDesigner[27] for the de novo design of anion receptors.[28] For instance, the creation of receptors for self-assembled cages[29a,h] and sulfate[29h] comprised of metals with geometry- and symmetry-matched ligands was made possible by recruiting known supramolecular synthons, such as hydrogen-bond donors[29b,c,e,h] and metal-binding sites,[29a,d] and utilizing the rules of symmetry to screen a database of linkers that could be used to connect them together.[29] The outcomes of this methodology are ligands that can be readily synthesized and that self-assemble directly into polyhedra with an ability to bind anions with matched shapes. An alternative method by Mascal involved the computer-aided design of a fluoride-selective receptor[30] capable of supporting anion–$\pi$ interactions that was later realized experimentally.[31] Finally, other prominent examples of computer-aided strategies applied to supramolecular host–guest complexes include Houk's extensive studies on gating in hemicarcerands.[32] Here, we take a complementary computer-aided-design approach to prescreen and then create anion receptors that can control the binding geometry of the bifluoride guest within the cavity of the triazolophane. This capability allows us to enhance the binding affinity of $HF_2^-$ to the macrocycle by altering the shape of the cavity and its electropositive character.

In our study, we focused on binding bifluoride using CH hydrogen bonds in a rigid two-dimensional macrocyclic triazolophane. We started with a study of the triazolophane 1 in the gas-phase (theory) and solution (experiment) to bind
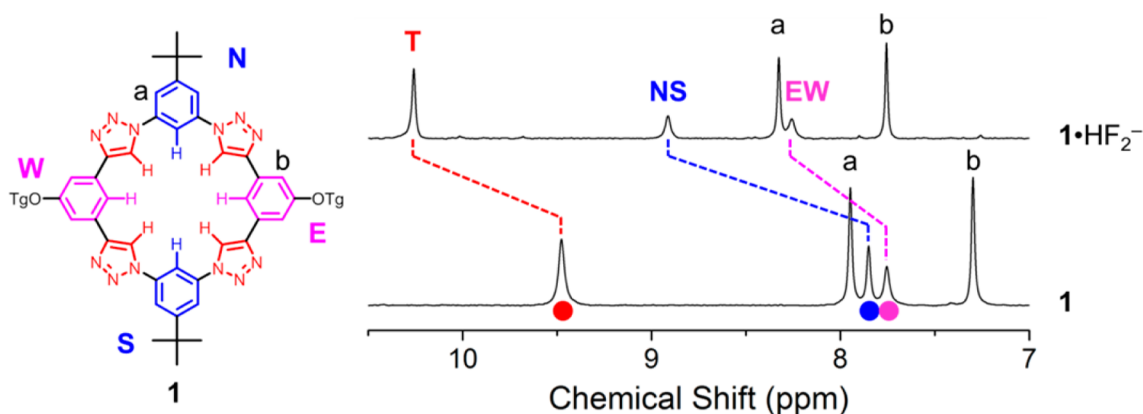
**Figure 1.** $^1$H NMR spectra (2 mM, CD$_2$Cl$_2$, 298 K, 500 MHz) of **1** and **1·HF$_2^-$** (35 equiv added). Triazole (**T**) protons (H$^T$) are colored in red, north−south (NS) phenylene protons (H$^N$) are blue, and east−west (EW) phenylene protons (H$^C$) are magenta.

bifluoride using the macrocycle's set of CH hydrogen-bond donors constituted by four extrinsically activated 1,2,3-triazoles and four phenylenes (Scheme 1). In order to correlate the results of calculations with experimental observations, we used the triazolophane's binding energies to Cl$^-$ for internal calibration. In the gas-phase calculations, we found the binding energies for both anions to be similar. Given the anion-to-cavity mismatch in shape and size (vide supra), HF$_2^-$ was found to be stable in multiple binding geometries. Among these, we noted a 20° tilting of the HF$_2^-$ anion out of the triazolophane's mean plane in the gas-phase calculations. We hypothesized that the tilting remained in solution and that it caused the reduction of the binding affinities relative to that of Cl$^-$. To test this idea, computer-aided design was employed to sift through three modifications that could be incorporated synthetically into the original triazolophane. The goal was to utilize modifications to the triazolophane that can minimize or remove the tilting angle of HF$_2^-$ as a means to improve the experimental binding affinity without having to synthesize a whole series of receptors in a trial and error approach. Consequently, this strategy accelerated greatly the design of macrocycle **2**. Experimental studies then yielded an enhanced bifluoride binding affinity which was found to be equal to that of Cl$^-$ in both the gas-phase calculations and as observed in the solution-phase experiments ($\sim 10^6$ M$^{-1}$).

## COMPUTATIONAL AND EXPERIMENTAL DETAILS

**DFT Calculations.** All computations have been carried out using the Gaussian suite of programs.[33] All the geometries have been optimized using the M06-2X functional.[34] In our previous study on cyanide binding,[3b] calculations performed on the parent tetraphenylene triazolophanes revealed that the use of a hydrogen atom in place of a methoxy group did not significantly affect the geometries and anion binding energies (<2 kcal/mol). On this basis, triazolophane **1** was modeled using **3** (Scheme 1), which has hydrogens in the place of the *tert*-butyl and triethylene glycol (OTg) groups. Macrocycle **2** was modeled by **4** (Scheme 1) with an alkoxy-linked OTg group replaced by an OH and the *tert*-butyl groups on the amide substituents truncated to hydrogens. All other macrocyclic models are truncated similarly with hydrogens. Vibrational frequencies, zero-point corrections, and thermal corrections have been evaluated using the 6-31+G(d,p) basis set. Unless stated, all the structures are confirmed to be minimum-energy structures with no imaginary frequencies. The basis set superposition errors (BSSE) on the computed interaction energies were evaluated using the standard counterpoise method.[35] Single-point energy calculations were carried out subsequently using the significantly larger 6-311++G(3df,2p) basis sets to obtain the anion

binding energies. Implicit solvent single-point computations were performed using the SMD model for the optimized geometries in the gas phase at the M06-2X/6-311++G(3df,2p) level of theory. Finally, Grimme's dispersion corrections to the M06-2X functional were also added to the computed energies, and the effects were found to be minimal (Supporting Information).

**NMR Titrations.** Titrations of macrocycles **1** and **2** with anions in the forms of tetra-*n*-butylammonium (TBA) salts were followed by $^1$H nuclear magnetic resonance (NMR) spectroscopy using a 500 MHz Varian Inova spectrometer at room temperature (298 K). In a typical experiment, 400 μL of 2 mM (or 0.5 mM) macrocycle solutions were prepared in screw-cap NMR tubes equipped with PTFE/silicone septa. Aliquots of 80 mM (or 20 mM) TBA salt solutions in scew-cap vials equipped with PTFE/silicone septa were added via 10 and 100 μL gastight microsyringes.

**UV−Vis Titrations.** Titrations using ultraviolet−visible (UV−vis) spectroscopy were conducted utilizing a Varian Cary 5000 UV−vis−NIR spectrophotometer at room temperature (298 K). Host solutions (5 μM, 4 mL) were prepared in 1 cm screw-cap quartz cell equipped with PTFE/silicone septa. Aliquots of 1 mM TBA salt solutions in scew-cap vials equipped with PTFE/silicone septa were added via 10 and 100 μL gastight microsyringes.

## RESULTS AND DISCUSSIONS

**Binding Modes of HF$_2^-$ in Triazolophanes.** Several different bifluoride−triazolophane binding modes can be envisioned. Binding can be along the north−south (NS), east−west (EW), or diagonal directions. A perpendicular mode of binding is also possible. The anion can either be nestled down in the plane of the macrocycle or oriented out of the plane.

$^1$H NMR titrations of **1** with tetrabutylammonium bifluoride (TBAHF$_2$) in CD$_2$Cl$_2$ were conducted to first evaluate the binding strength and the likely binding modes. The chemical shifts of all the triazolophane protons observed during the $^1$H NMR titration (Figure 1) with bifluoride indicate binding.[2] In particular, the inner protons (H$^T$, H$^N$, and H$^C$) have noticeable downfield movements consistent with significant hydrogen-bond interactions between triazolophane **1** and bifluoride. Both the chemical shifts and peak widths stop changing following addition of 35 equiv of TBAHF$_2$, indicating that triazolophane **1** is presumably saturated as the 1:1 complex, **1·HF$_2^-$**. Upon HF$_2^-$ binding, the protons H$^N$ along the north−south axis displayed the largest shift (1.1 ppm), which were more than twice as large as that of the H$^C$ (0.5 ppm) located along the east−west axis. By contrast, the complexation-induced chemical shifts (Δδ, Figure 2) of the three inner protons (H$^N$, H$^C$, and
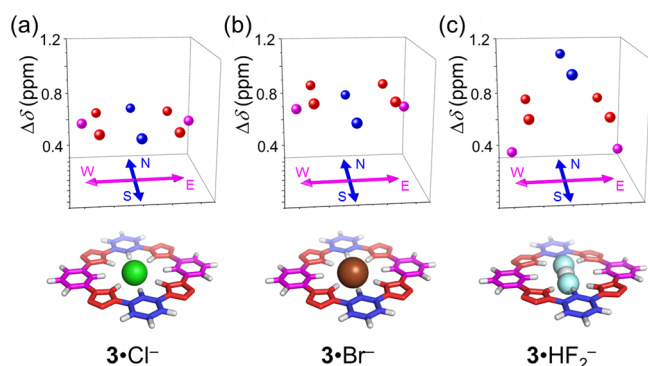
**Figure 2.** Representation of the complexation-induced chemical shifts ($\Delta\delta$, vertical axis) for triazolophane **1** versus spatial location of each inner proton upon binding (a) Cl$^-$,[2b] (b) Br$^-$,[2b] and (c) HF$_2^-$. The shifts for triazole protons (**T**) are colored in red, those of north–south (NS) phenylene protons (H$^N$) are blue, and those of east–west (EW) phenylene protons (H$^C$) are magenta. Structures of anion complexes for **3** were optimized with M06-2X/6-31+G(d,p).

H$^T$) in the symmetrically bound halide complexes,[2b] such as **1**·Cl$^-$ and **1**·Br$^-$, are all similar (ca. 0.8 ppm). Since the shapes of the rigid tetraphenylene triazolophanes change very little upon anion binding,[3a] these results indicate that bifluoride prefers to bind along the NS direction. This outcome matches with our previous theoretical[3a] and experimental[3b] findings that the nitrogen-linked phenylenes, located along the north–south axis in **1**, allow for greater stabilization of anions than the carbon-linked ones located east–west.

The binding modes were also examined by gas-phase calculations utilizing a simplified triazolophane, **3** (Figure 3),
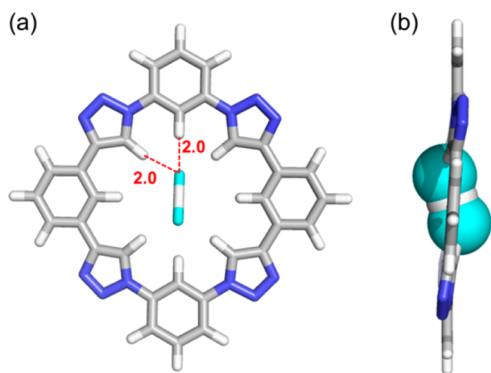


**Figure 3.** Hydrogen-bonded distances (red, Å) in **3**·HF$_2^-$ in (a) front view and (b) side view. The structure of the complex is optimized with M06-2X/6-31+G(d,p).

with hydrogen atoms in place of solubilizing substituents (OTg or *tert*-butyl group). The fully coplanar, $D_{2h}$-symmetric form of the bifluoride complex **3**·HF$_2^-$ in the NS binding geometry was investigated first. It turns out to be a second-order saddle point. Its two imaginary frequencies correspond to the puckering of the macrocycle and a tilting motion of the bifluoride out of plane with retention of the north–south binding direction. The optimized structure obtained after perturbing along these imaginary frequencies has $C_{2h}$-symmetry wherein the bifluoride is tilted ca. 21° relative to the triazolophane's mean plane and the bifluoride's hydrogen atom is situated perfectly at the complex's center of mass. The two northern triazole protons (H$^T$) are seen to point up toward one of the bifluoride's

fluorine atoms and the two southern triazoles point down toward the other fluorine (Figure S11, Supporting Information). Both the north–south phenylene protons and all four triazole protons engage (Figure 3) the terminal fluorines of bifluoride with six short CH···F hydrogen bonds (ca. 2.0 Å). Interestingly, these distances are comparable to the NH···F contacts (1.8–2.0 Å) seen in the crystal structure of the caged HF$_2^-$ complex reported by Bowman-James.[6a]

The fully planar $D_{2h}$-symmetric complex with bifluoride oriented along the EW direction is also a second-order saddle point. Perturbing along its imaginary frequencies results in the $C_s$-symmetric complex **3**·HF$_2^-$ (Figure S11, Supporting Information) again with a ca. 21° tilting angle. The hydrogen-bond distances in the EW mode resemble those from the NS mode (Table S2, Supporting Information), i.e., short 2 Å contacts. We believe that this binding mode is also present in solution and it accounts for the 0.5 ppm migration in the east–west protons upon bifluoride complexation (Figure 1).

Since both the NS and EW binding modes were found to be minimum-energy structures of **3**·HF$_2^-$, we were curious about the nature of the other binding modes. For instance, HF$_2^-$ could potentially be pointed diagonally toward the triazoles (**T**). Structural optimization produces a $C_i$-symmetric **3**·HF$_2^-$ structure with one imaginary frequency. Perturbation along one direction of the imaginary normal mode leads to the NS binding arrangement and to the EW geometry in the other direction. This diagonal structure thus appears to be the transition state for the in-plane precessional interconversion between the two local minima (Figure 4). Finally, the perpendicular bifluoride binding mode, with the bifluoride bisected by the macrocycle's mean plane, is found to be a higher-order saddle point with several imaginary frequencies. Systematically perturbing each of these imaginary frequencies eventually results in the NS and EW modes as the only two
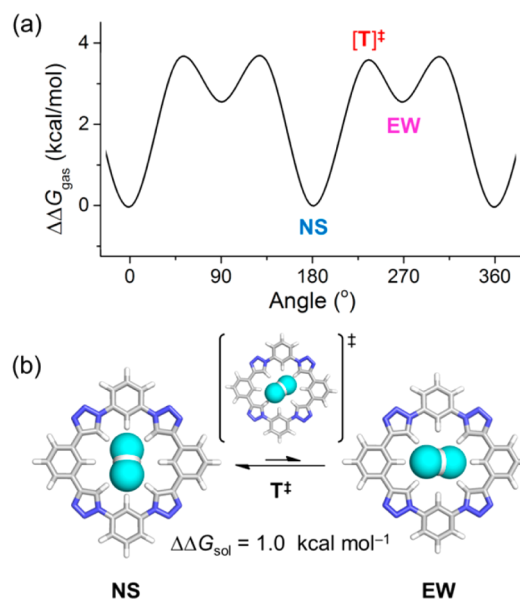


**Figure 4.** (a) Free energy profile of HF$_2^-$ gyrating inside the cavity of triazolophane **3** starting from one of the two degenerate NS modes (0°). The geometry was optimized with M06-2X/6-31+G(d,p) and energy calculations were optimized with M06-2X/6-311++G(3df,2p). (b) Structures of the precessional states and the transition state. The energy difference in solution phases in favor of the NS mode is calculated from experiment (dichloromethane).
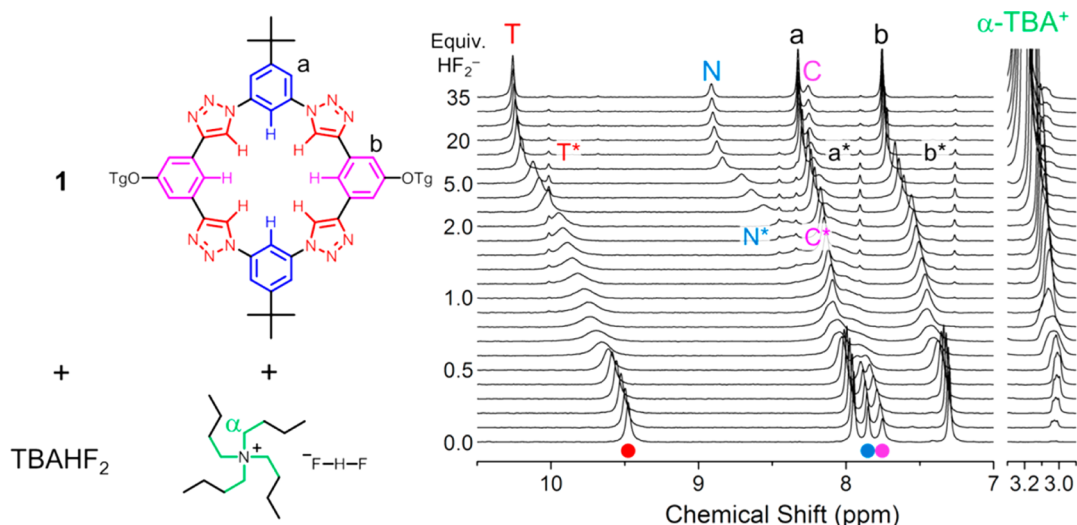
**Figure 5.** ^{1}H NMR titration (2 mM, CD$_2$Cl$_2$, 298 K, 500 MHz) of **1** with increasing equivalents of TBAHF$_2$. The signal of the triazole (**T**) proton (H$^T$) is labeled in red, that of north−south (NS) phenylene proton (H$^N$) in blue, that of east−west (EW) phenylene protons (H$^C$) in magenta, and that of α-TBA$^+$ protons in green. Proton peaks associated with **1$_2$·SiF$_6$$^{2−}$** are labeled with * (see the explanation in the text).

minima. The hydrogen-bonding distances (H$^T$···F, 2.8 Å; H$^N$···F, 3.1 Å; H$^C$···F, 3.2 Å) in the complex with bifluoride bound in a perpendicular manner are larger than the sum of the van der Waals radii (2.7 Å). Consequently, it is not surprising that the binding free energy of this state is one-third less than that of the others.

Overall, the different optimized structures of **3·HF$_2$$^−$** obtained using computation are consistent with our experimental findings in the solution phase that the NS geometry represents the dominant mode of bifluoride binding.

**Precessional Motion of HF$_2$$^−$ in Triazolophanes.** As mentioned above, the NS binding geometry was found to be the global minimum with the EW mode lying 2.5 kcal mol$^{−1}$ higher in energy. The population of each geometric arrangement is expected to be a Boltzmann average. The free energy barrier between the NS and EW complexes via the proposed transition state, **T$^‡$**, was calculated to be 3.6 kcal mol$^{−1}$ at room temperature. This energy barrier is within the range for a C−C rotation (3−5 kcal mol$^{−1}$),[36] and therefore, the precessional movements of HF$_2$$^−$ within the binding cavity are "free rotors" at room temperature. Consequently, we expect the exchange between minima to occur much faster than the NMR time scale.

Since the phenylene hydrogen atoms have similarly short hydrogen-bond distances (ca. 2 Å) in the NS and EW modes, the greater shift in the north−south proton's NMR resonance indicates that the NS mode is more populated in solution. To evaluate the energy difference, $\Delta\Delta G_{sol}$, between NS and EW binding modes, we applied the Boltzmann distribution shown in eq 2

$$g_i N_i / g_j N_j = \exp(-\Delta E_{ij}/k_B T) \qquad (2)$$

where $k_B$ is the Boltzmann constant, $T$ is the temperature, $g$ is the degeneracy of levels having energy $E$, and $N$ is the population. Calculations indicate that the degeneracies are different in the NS and EW modes (Figure S12, Supporting Information). In the NS binding mode, *two* degenerate states were found, while in EW there are *four* on account of the fact that there is a 0.3 Å displacement of HF$_2$$^−$ away from the center of mass of the triazolophane. Consequently, the $\Delta\Delta G_{sol}$ was

estimated to be 1.0 ± 0.1 kcal mol$^{−1}$ with a population distribution of 74% in the two NS modes and 26% in the four EW modes [Figures 3b and S13 and Tables S3, S4 (Supporting Information)]. The difference is smaller than in the gas phase, which we attribute to solvation. Computations using an implicit solvation model (see Supporting Information) are consistent with the ~1 kcal mol$^{−1}$ difference between the two binding modes.

**Solution Binding Affinity of HF$_2$$^−$ with Triazolophane 1.** [1]H NMR titrations of **1** with TBAHF$_2$ in CD$_2$Cl$_2$ (Figure 5) were utilized to establish the dominant equilibria present at millimolar concentrations. In dichloromethane, ion pairing between the cation (TBA$^+$) and the anionic species are usually significant.[25] Since the chloride salt TBACl has an ion-pair association constant ($K_{ip}$) similar to that of TBAHF$_2$ (see Supporting Information), the ion-pair complex (**1·HF$_2$$^−$·TBA$^+$**) between TBA$^+$ and the 1:1 anionic complex was also included. Unexpectedly, the ^{1}H NMR peaks of the TBA$^+$ cation, e.g., α-methylene proton, were found to shift slightly upfield initially and then turn downfield after the addition of just 0.5 equiv of bifluoride (Figure S9, Supporting Information) rather than at 1.0 equiv, as seen with chloride titrations.[25] On the basis of our previous studies,[25] we attribute this phenomenon to pairing of the cation with the 2:1 complex to produce **1$_2$·HF$_2$$^−$·TBA$^+$**. The significant peak broadening seen at 0.5 equiv in the ^{1}H NMR spectra is consistent with the existence of higher-order species.

While the formation of 2:1 ion-pair complexes with triazolophane has been previously hypothesized,[25] the observation described above is the first direct solution-phase evidence for this species. To rationalize its presence, we compared the HF$_2$$^−$ binding behavior to that previously seen with spherical halides. When a 2:1 species is formed with halides, the structure of the sandwich complexes[2c] is expected to shield the encapsulated anion from forming further intermolecular contacts. By comparison, the tilted conformation of bifluoride within the 1:1 complex could presumably be inherited by the 2:1 complex. Even though the structure of the 2:1 complex is prohibitively large to be accurately optimized using DFT calculations, we propose a binding mode where each macrocycle interacts with one fluorine terminus of the tilted HF$_2$$^−$ (2:1 complexes in Figure 6), and its linearity points
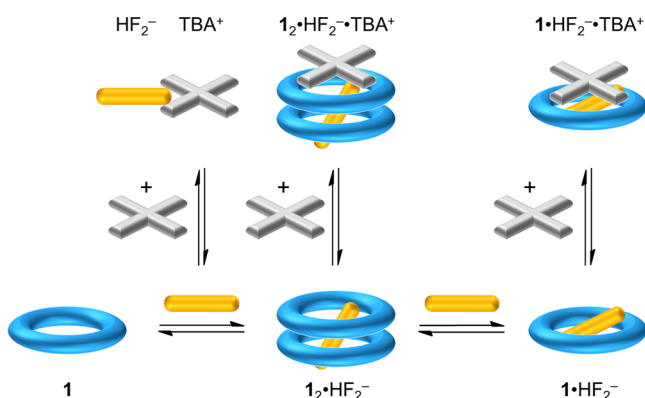
**Figure 6.** Cartoons showing solution-phase equilibria associated with triazolophane **1** binding $HF_2^-$ (2 mM, $CD_2Cl_2$, 298 K).

negative electron density into solution. Consequently, $HF_2^-$ in the sandwiched complex is still able to attract the TBA$^+$ cation as a 2:1 ion pair complex.
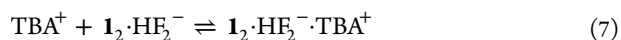
To further support our model, we monitored how the prevalence of each species changes with concentration. Upon dilution from 2 to 0.5 mM, the turning point of the $\alpha$-methylene proton's $^1$H NMR signal moved toward 1.0 equiv, which indicates that the 2:1 ion pair complex $\mathbf{1}_2 \cdot HF_2^- \cdot TBA^+$ is being diluted away and the 1:1 ion pair complex $\mathbf{1} \cdot HF_2^- \cdot TBA^+$ becomes the dominant ion-pair complex.

In addition, a minor species (asterisks in Figure 5) was observed in the $^1$H NMR titration. Multiple characterization methods confirmed the emergence and disappearance of a sandwich complex involving the hexafluorosilicate dianion, $\mathbf{1}_2 \cdot SiF_6^{2-}$ (see Supporting Information). The presence of this silicate has been reported in the literature[37] and was attributed to the reaction between fluoride species, the glass walls, and a proton source. In our case, $HF_2^-$ is a capable etchant by itself (see Supporting Information). Overall, the observations of the $^1$H NMR titrations led us to the binding model of eqs 3–8:
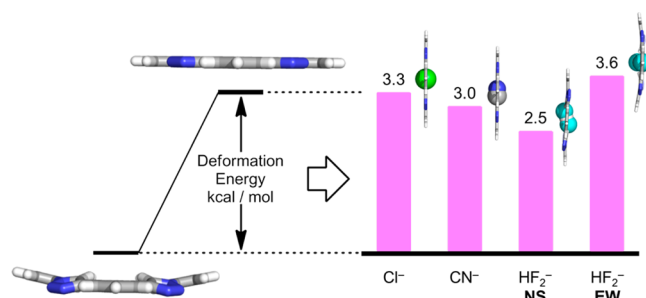
Complexation:

$$\mathbf{1} + HF_2^- \rightleftharpoons \mathbf{1} \cdot HF_2^- \tag{3}$$

$$\mathbf{1} \cdot HF_2^- + \mathbf{1} \rightleftharpoons \mathbf{1}_2 \cdot HF_2^- \tag{4}$$

Ion-pairing:

$$TBA^+ + HF_2^- \rightleftharpoons TBAHF_2 \tag{5}$$

$$TBA^+ + \mathbf{1} \cdot HF_2^- \rightleftharpoons \mathbf{1} \cdot HF_2^- \cdot TBA^+ \tag{6}$$

$$TBA^+ + \mathbf{1}_2 \cdot HF_2^- \rightleftharpoons \mathbf{1}_2 \cdot HF_2^- \cdot TBA^+ \tag{7}$$

Binding of $SiF_6^{2-}$:

$$\mathbf{1} + \mathbf{1} + SiF_6^{2-} \rightleftharpoons \mathbf{1}_2 \cdot SiF_6^{2-} \tag{8}$$

Fortunately, this menagerie of complexes can be greatly simplified by diluting out the weaker equilibria[38] at lower concentration. Consequently, the 1:1 binding of $HF_2^-$ with **1** can be accurately determined by fitting the UV–vis titration data (see Supporting Information) in $CH_2Cl_2$ (Table 1) using an equilibrium-restricted factor analysis on the entire wavelength range (250–340 nm) of data with Sivvu.[39] At 0.5 $\mu$M, equilibria involving higher-order species (eqs 4, 6, 7, and 8) can be safely removed from the solution binding model (see Supporting Information), leaving us to determine the association constant for eq 3 after independently measuring ion-pairing (eq 5). The 1:1 $HF_2^-$ binding affinity (290 000 ± 10 000 $M^{-1}$) was found to be more than 1 order of magnitude lower than that of chloride (7 400 000 ± 700 000 $M^{-1}$).[2d]

**Rationale for Decreased $HF_2^-$ Binding Affinity in Solution.** Examining the difference between $HF_2^-$ and the other anions that have been previously studied[3] helped us to rationalize the lowering of the bifluoride binding affinity in solution relative to $Cl^-$. Triazolophane **1** normally flattens out its ruffled conformation when chloride,[3a] bromide,[3a] or cyanide[3b] is bound. Upon $HF_2^-$ binding, however, both the NS and EW modes remain ruffled. Deformation energies[40] can be used to evaluate whether $HF_2^-$ binding gives rise to a larger penalty (Figure 7). The deformation energy for $HF_2^-$ is actually



**Figure 7.** Deformation energies of triazolophane **3** (side view) for binding to the different anions. The energies are calculated by M06-2X/6-311++G(3df,2p).

the lowest (2.5 kcal mol$^{-1}$) among the NS complexes, even after taking the 74:26 Boltzmann distribution into account (~2.8 kcal mol$^{-1}$). Thus, the possibility that a larger deformation penalty is associated with $HF_2^-$ binding can be excluded.

The counterintuitive fact that three different anions, $Cl^-$, $CN^-$, and $HF_2^-$, each have very similar binding energies with **3** in gas-phase calculations regardless of their orientations or

**Table 1. Calculated and Experimental Binding Energies of Triazolophanes with $Cl^-$ and $HF_2^-$ According to Eq 3**

| | $3^a$ | 1 | | $4^a$ | 2 | |
|---|---|---|---|---|---|---|
| | $\Delta G°_{gas}$ (kcal mol$^{-1}$) | $\Delta G_{soln}$ (kcal mol$^{-1}$) | $K_{soln}$ ($\times 10^5$ M$^{-1}$) | $\Delta G°_{gas}$ (kcal mol$^{-1}$) | $\Delta G_{soln}$ (kcal mol$^{-1}$)$^d$ | $K_{soln}$ ($\times 10^5$ M$^{-1}$) |
| $Cl^-$ | −55 | −9.4 ± 0.1$^b$ | 74 ± 7 | −59 | −7.4 ± 0.1 | 3.0 ± 1.0 |
| $NS \cdot HF_2^-$ | −53 | −7.5 ± 0.1$^c$ | 2.9 ± 0.1 | | | |
| $EW \cdot HF_2^-$ | −50 | | | −57 | −7.9 ± 0.1 | 6.2 ± 1.2 |
| $[\mathbf{D} \cdot HF_2^-]^{\ddagger}$ | −49 | | | | | |

$^a$Counterpoise corrected at M06-2X/6-311++G(3df,2p). $^b$Data reported in refs 2b and 2d were re-evaluated by including the formation of an ion-pair complex and a 2:1 complex. $^c$Determined by UV–vis titration ($CH_2Cl_2$, 0.5 $\mu$M). $^d$Determined by UV–vis titration ($CH_2Cl_2$, 5 $\mu$M)

5083

dx.doi.org/10.1021/ja500125r | *J. Am. Chem. Soc.* 2014, 136, 5078–5089

hydrogen-bond configurations led us to an alternative hypothesis: When the anion is tilted, e.g., $HF_2^-$ (Figure 8),
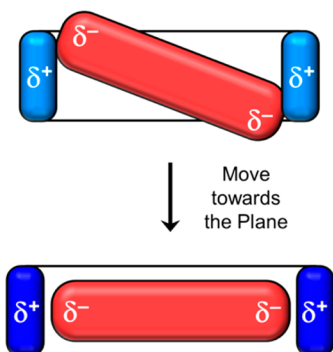


**Figure 8.** Cartoon representations of tilted and coplanar $HF_2^-$ inside a macrocycle. $HF_2^-$ is represented by a red, cylindrical rectangle with two electronegative ends. The cross-section of a generic macrocycle is represented by a box with two electropositive sites in blue, indicating hydrogen-bond donors.

the negatively charged termini of the anion are more exposed to solvent. Solvation can then more effectively stabilize the excess charge on the anion and reduce its availability for hydrogen bonding. Furthermore, the dielectric effect significantly reduces the ionic contribution to the hydrogen bond between the triazole CH and the fluorines from $HF_2^-$. These features might explain why $Cl^-$ and $HF_2^-$ are equally bound in gas-phase calculations but they differ markedly in solution-phase characterization. Computations were then performed to complement our hypothesis. Interestingly, the gas-phase calculations suggest that $HF_2^-$ binding of **3** ($\Delta G^{\circ}_{gas}$ = −53 kcal mol$^{-1}$) is just as strong as $Cl^-$ binding (−55 kcal mol$^{-1}$). However, after including implicit solvation, the calculations qualitatively reproduced the experimental results. That is, chloride binding (computed $\Delta G_{soln}$ = −8 kcal mol$^{-1}$) was found to be much stronger than that of bifluoride (computed $\Delta G_{soln}$ = −3 kcal mol$^{-1}$).

**Computer-Aided Design of New Macrocyclic Receptors.** The tilting of $HF_2^-$ within the cavity of **1** is believed to be responsible for its lower binding affinity. Consequently, a redesign of the receptor was considered as a means to generate a nontilted binding mode (Figure 8). This geometric factor is expected to enhance the $HF_2^-$ affinity and to ensure that its binding is equal to that of $Cl^-$ in both gas and solution phases. Elongated designs,[6b] which have been shown to have good binding with linear anions, e.g., $N_3^-$ and $HF_2^-$, are not appropriate candidates, as these receptors usually weakened $Cl^-$ affinity due to the size mismatch. In order to best test our hypothesis, new molecular designs are needed where two criteria are met: (1) $HF_2^-$ is bound nontilted and (2) similar binding affinity exists toward $Cl^-$ and $HF_2^-$. The second criterion allows the impact of the tilting behavior on solution binding affinities to be verified; if $HF_2^-$ is bound in a nontilted mode, we would then observe similar binding affinity to $Cl^-$ in solution. While it is not feasible to determine the tilting angle of a bound $HF_2^-$ by observation, we employed computer-aided design on a series of triazolophanes and monitored the resulting tilting angle within the structurally optimized complex (Figure 9).

The first feature investigated was size- and shape-matching. The rigidity of the triazolophane was relaxed slightly by
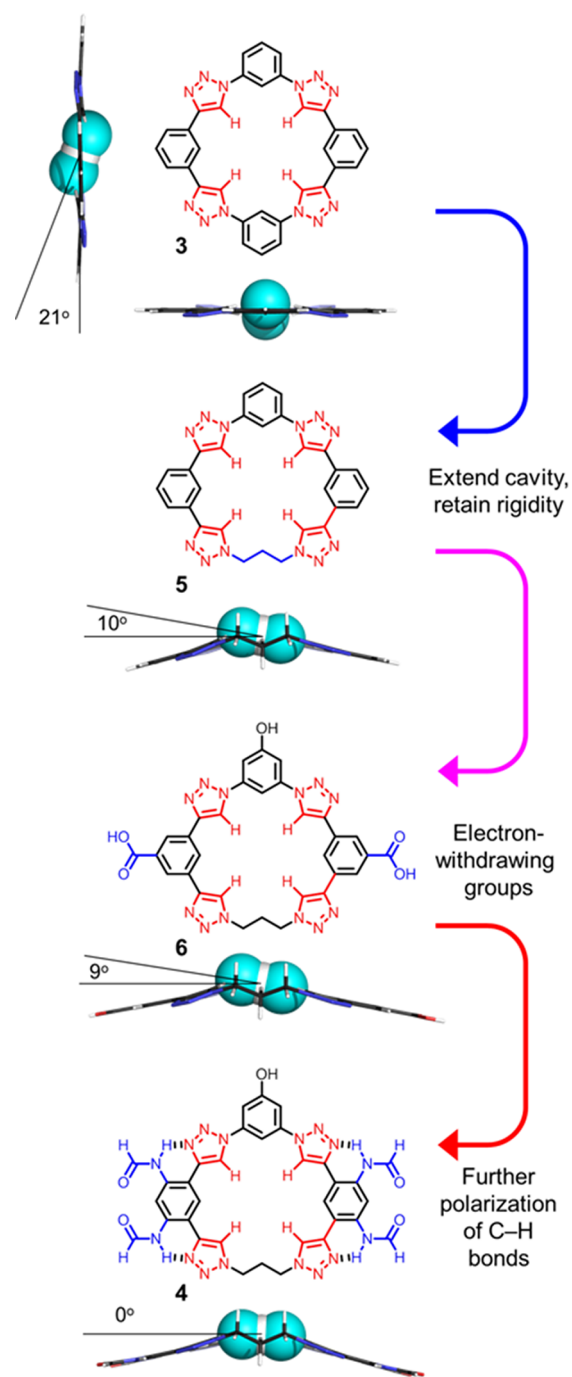


**Figure 9.** Chemical structures of macrocycles **4−6** and their molecular design features based on **3**. Optimized structures using M06-2X/6-31+G(d,p) of **3−6** are oriented in EW side views.

incorporating a flexible 1,3-propylene linker, thereby allowing triazolophane **5** to accommodate a slightly larger anion. Prior work with this substitution showed a negligible lowering of the triazolophane's $Cl^-$ affinity.[2f] Consistent with our expectations, structural optimization of its EW mode showed a ~50% reduction in the tilting angle to 10°. In addition, the cavity size along the east−west axis became 0.4 Å larger than that of the NS mode, suggesting that the EW mode in triazolophane **5** may now be preferred by $HF_2^-$.

The second strategy involved tuning the electronics by adding carboxylic acid as electron-withdrawing groups onto the EW phenylenes. In addition, a hydroxyl group was introduced

to the north phenylene to mimic any glycol ether chains that would be needed for solubility. However, calculations on triazolophane **6** yielded no significant improvement. Presumably, the inductive effect of esters is too weak to affect the electropositive character of triazole protons. An insignificant change in cavity size for the EW and NS modes was observed, which may also reflect the minimal change in electronics (Table S4, Supporting Information).

To more significantly enhance the electropositive character of the cavity, four flanking amides were introduced onto the phenylenes along the east–west axis to yield amide triazolophane **4**. The intramolecular NH···N hydrogen bonds formed between amide NH donors, and the four triazoles were previously discovered to polarize CH donors.[26] As computational studies have shown, the cavity size of **4** is further expanded so that the length along the EW is 0.8 Å larger than that of the NS. The expansion of the cavity along the east–west direction may have resulted from the increased repulsions between the more electropositive triazole protons. Interestingly, the largest dimension of the pocket along the east–west axis of **4** ($r$ = 3.9 Å) is only 0.3 Å larger than that of triazolophane **3** and is still smaller than the van der Waals radius of $HF_2^-$ along the F–H–F axis ($r$ = 5.3 Å). With this macrocycle, we verified computationally that the desired tilt-angle of 0° was achieved. The nontilted conformation of $HF_2^-$ binding with triazolophane **4** is attributed to the enhanced attraction between **4** and $HF_2^-$ (Figure 10). The enhancement
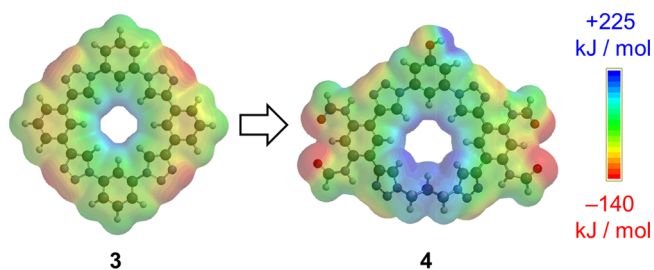
coincides with the ~30 kJ mol$^{-1}$ increase in the maximum electrostatic potential (B3LYP/6-31+G*) inside the cavity from 225 kJ mol$^{-1}$ for **1** to 255 kJ mol$^{-1}$ for **4**. Finally, gas-phase calculations showed that the binding energies between macrocycle **4** and Cl$^-$ and $HF_2^-$ are equal (Table 1). These attributes marked **4** as a suitable target molecule for further experimental binding studies.

Overall, by using computer-aided design we examined how various molecular design features could impact the binding geometry of bifluoride. Elongation alone, by introducing a propylene linker, was insufficient to accommodate bifluoride anion in **5**. Neither will the enhanced electropositive character improve the performance if the substituents are introduced on the wrong positions. Installing electron-withdrawing groups in the EW phenylenes in **6** fails to provide significant improvement, although their CH groups are linearly aligned with the bound bifluoride in the local minimum structure. Use of electron-withdrawing amides groups on the phenylenes that also interact directly with the triazoles has a much better performance. This observation indicates that the binding energy and geometry is largely dependent on the triazoles' interactions with the anion. Even then, in triazolophane **4**, the size and shape are still mismatched: the length of bifluoride is ~1 Å larger than the length of the cavity along the EW direction; the aspect ratio of the cavity between the EW and NS directions is ~1.1, i.e., almost spherical. Therefore, the subtle elongation in EW directions (~0.4 Å) must cooperate positively with the enhanced electropositive character (~30 kJ mol$^{-1}$) in **4** to allow the bifluoride anion to be bound in plane and without any tilting.

**Solution Binding Studies of $HF_2^-$ in Triazolophane 2.** The semirigid macrocycle **2** was synthesized[2b] as the experimental analog of **4** to test the effectiveness of the computer-aided design (Scheme S1, Supporting Information). $^1$H NMR titrations of **2** were performed with TBAHF$_2$ (Figure 11) and TBACl (Figure 12) in CDCl$_3$. In the Cl$^-$ titrations, the 2:1 complex persists (red boxes, Figure 12), and it requires ca. 6 equiv of Cl$^-$ to shift the preferences to favor the 1:1 complex.



**Figure 10.** Electrostatic potential maps of triazolophanes **3** and **4**.



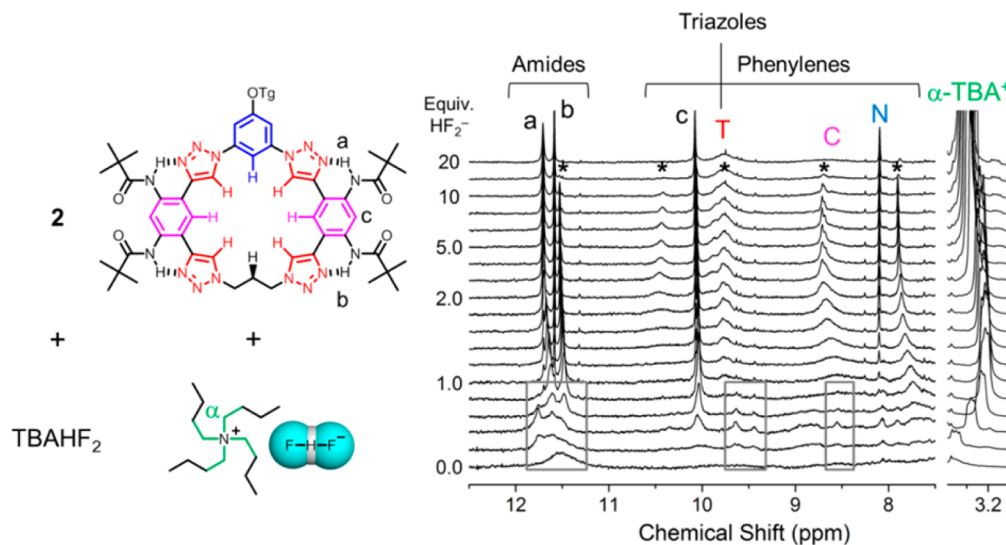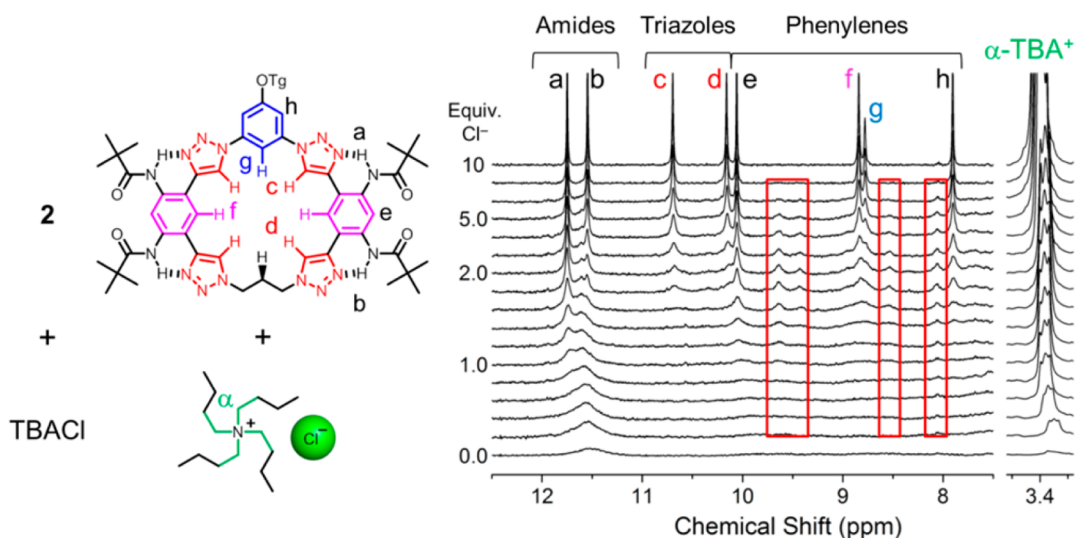**Figure 11.** $^1$H NMR titration (2 mM, CDCl$_3$, 298 K) of **2** with increasing equivalents of TBAHF$_2$. The signal of the triazole protons (H$^T$) is labled in red, that of north phenylene proton (H$^N$) in blue, and that of EW phenylene protons (H$^C$) in magenta. **2**$_2$·SiF$_6^{2-}$ is labeled with asterisks. **2**$_2$·HF$_2^-$ is shown in gray boxes.

**Figure 12.** $^1H$ NMR titration (2 mM, CDCl$_3$, 298 K) of **2** with increasing equivalents of TBACl. The signal of the triazole protons (H$^T$) is labeled in red, that of north phenylene proton (H$^N$) in blue, and that of EW phenylene protons (H$^C$) in magenta. **2**$_2\cdot$Cl$^-$ is shown in red boxes.
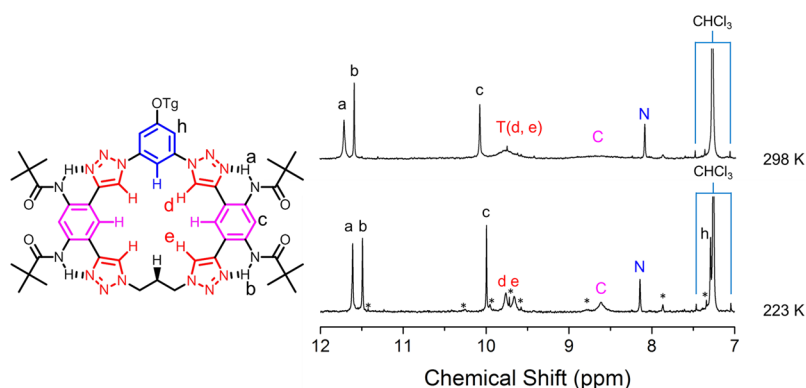


**Figure 13.** Low-temperature $^1H$ NMR spectra of macrocycle **2** (2 mM) in CDCl$_3$ with TBAHF$_2$ (20 equiv, 400 MHz, 223 and 298 K). Silicate complex **2**$_2\cdot$SiF$_6^{2-}$ was promoted by lowering the temperature and is marked with asterisks.

In comparison to the parent triazolophane, the overall formation ($\beta \sim 10^9$) of the 2:1 complex (gray boxes, Figure 11) was determined to be 1 order of magnitude weaker. The bifluoride anion inside the 2:1 species is instead replaced by silicate with the formation of **2**$_2\cdot$SiF$_6^{2-}$ seen from 1.6 to 15 equiv as marked by the asterisks in Figure 11. The silicate sandwich complex is ultimately replaced by the 1:1 bifluoride complex beyond 15 equiv of HF$_2^-$.

The formation of ion pairs is still observed in chloroform and included in the binding models. A significant turning point observed in the $\alpha$-methylene proton of TBA$^+$ upon HF$_2^-$ addition (Figure 11) and a more subtle turning point in the case of TBACl (Figure 12) are both seen at ca. 1.0 equiv. For the Cl$^-$ titration, the higher population of the 2:1 sandwich complex at 1.0 equiv reduced the significance of the 1:1 ion-pair complex (Figure S32, Supporting Information). These features are summarized by the following equilibria (X = HF$_2^-$ or Cl$^-$):

Complexation:

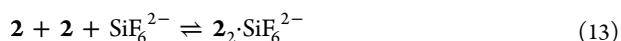$$2 + X^- \rightleftharpoons 2\cdot X^- \tag{9}$$

$$2\cdot X^- + 2 \rightleftharpoons 2_2\cdot X^- \tag{10}$$

Ion-pairing:

$$TBA^+ + X^- \rightleftharpoons TBAX \tag{11}$$

$$TBA^+ + 2\cdot X^- \rightleftharpoons 2\cdot X^-\cdot TBA^+ \tag{12}$$

Binding of SiF$_6^{2-}$:

$$2 + 2 + SiF_6^{2-} \rightleftharpoons 2_2\cdot SiF_6^{2-} \tag{13}$$

Upon saturation with HF$_2^-$, the triazole (H$^T$) and phenylene protons (H$^C$) remained broadened into the baseline, indicative of the dynamics associated with the bound bifluoride. These peaks can be resolved by lowering the temperature (Figure 13) with the two inequivalent triazole peaks, H$^d$ and H$^e$, now evident. Interestingly, phenylene proton (H$^N$) in the north behaves distinctly differently from the similar north–south protons in **1** (Figure 5) and the other hydrogen-bonded protons in **2** (H$^T$ and H$^C$): It remains sharp throughout the titration. Therefore, H$^N$ is not participating in the dynamic behavior and it likely has a small role to play in stabilizing HF$_2^-$. The very small complexation-induced chemical shift of H$^N$ associated with **2**$\cdot$HF$_2^-$, which is 0.7 ppm smaller than that in chloride complex, supports this last idea. These observations suggest that the bound bifluoride has been locked into the EW binding mode, presumably as a result of three factors: (1) The NS cavity is now much smaller than the EW one; (2) the nontilted EW binding mode results in HF$_2^-$ occupying the cavity so that the solvent effect is neutralized; and (3)

polarization of the CH bonds along the EW direction shifts the orientational preference of bound $HF_2^-$ away from the original NS mode. Having created a binding mode that we believe is more competent for bifluoride, we are in a position to test our hypothesis that the solution binding will be consistent with the gas-phase calculation, i.e., the binding affinity of triazolophane **2** with $HF_2^-$ is expected to match the $Cl^-$ affinity in both gas and solution phases.

The 1:1 binding affinities of $HF_2^-$ and $Cl^-$ with triazolophane **2** were quantitatively determined by equilibrium-restricted factor analysis of the UV−vis titrations $(CH_2Cl_2, 5 \mu M$, Table 1).[41] The 1:1 $HF_2^-$ binding energy $(-7.9 \pm 0.1 \text{ kcal mol}^{-1})$ was found to match the $Cl^-$ binding affinity with **2** $(-7.4 \pm 0.1 \text{ kcal mol}^{-1})$. This similarity demonstrates that the tilted binding model can account for the reduced binding affinity of $HF_2^-$ to the parent tetraphenylene triazolophane macrocycles, like **1**, in solution phases. The computer-aided molecular design can successfully reinforce the binding strength of $HF_2^-$ to triazolophane macrocycles.

The only three previous studies[6−8] on bifluoride binding showed how the anion can be bound in the oval-shaped cavities of neutral receptors[6] and the $Li^+$ in charged receptors[7] and the fact that bifluoride can compete with the binding of fluoride. Our study reveals for the first time how bifluoride can also be bound in a mismatched host like **1**. In contrast to previous studies, where conclusions were established by varying the guests, we took a complementary approach by modifying the structure of the host. Herein, a new lesson in receptor design is thus learned: *the binding affinity of bifluoride does not depend entirely on size and shape matching*. In the gas phase, where only the host−guest interactions are considered, bifluoride was shown to be bound with the same affinity as chloride, albeit in a tilted geometry as a result of shape and size mismatch. In solution, however, a completely different story ensues. Computer-aided design was then used to inspect the role of solvent, where the tilting was examined in different macrocycles and was eventually removed in the final design. Overall, we learn that the tilting of bifluoride is a compromise between minimizing the hard sphere repulsions between the bifluoride anion and the macrocycle cavity and maximizing the anion's hydrogen-bond interactions with the triazoles.

## CONCLUSIONS

Computer-aided molecular design was shown to accelerate the creation of a new anion receptor capable of complexing the often overlooked, yet surprisingly common, bifluoride anion in a nontilted arrangement with high strength. This binding geometry was believed to be critical for keeping the binding energy high by preventing solvent-induced destabilization of the complex. In the parent triazolophane, with its spherical cavity, calculations show that the bifluoride is tilted while the shape-matched chloride fits snugly inside. In this case, the gas-phase affinity is the same for both anions, but it is not so in solution, where $HF_2^- < Cl^-$. When the triazolophane is customized to allow the bifluoride complex to mimic the chloride's coplanar geometry, their stabilities are observed to equalize, $HF_2^- \approx Cl^-$. Interestingly, the bifluoride was bound with reasonable strength, indicating that it could compete for receptor binding whenever fluoride is present. These findings indicate that future fluoride-based studies of binding should take these chemical species into consideration.

## ASSOCIATED CONTENT

**S** **Supporting Information**

Computational methods, syntheses, NMR data, optimized structures, UV−vis data, and titration analyses. This material is available free of charge via the Internet at http://pubs.acs.org.

## AUTHOR INFORMATION

**Corresponding Author**
kraghava@indiana.edu; aflood@indiana.edu

**Author Contributions**
[†]R.O.R. and Y.L. contributed equally.

**Notes**
The authors declare no competing financial interest.

## REFERENCES

(1) Sessler, J. L.; Gale, P. A.; Cho, W.-S. *Anion Receptor Chemistry*; RSC Publishing: Cambridge, U.K., 2006.

(2) Synthesis and anion binding studies of tetraphenylene triazolophanes: (a) Li, Y.; Flood, A. H. *Angew. Chem., Int. Ed.* **2008**, *47*, 2649−2652. (b) Li, Y.; Flood, A. H. *J. Am. Chem. Soc.* **2008**, *130*, 12111−12122. (c) Li, Y.; Pink, M.; Karty, J. A.; Flood, A. H. *J. Am. Chem. Soc.* **2008**, *130*, 17293−17295. (d) Li, Y.; Vander Griend, D. A.; Flood, A. H. *Supramol. Chem.* **2009**, *21*, 111−117. (e) Hua, Y.; Flood, A. H. *Chem. Soc. Rev.* **2010**, *39*, 1262−1271. (f) Hua, Y.; Ramabhadran, R. O.; Karty, J. A.; Raghavachari, K.; Flood, A. H. *Chem. Commun.* **2011**, *47*, 5979−5981. (g) McDonald, K. P.; Hua, Y.; Lee, S.; Flood, A. H. *Chem. Commun.* **2012**, *48*, 5065−5075. (h) Lee, S.; Flood, A. H. *Top. Heterocycl. Chem.* **2012**, *28*, 85−107.

(3) Computational studies of anion binding with tetraphenylene triazolophanes: (a) Bandyopadhyay, I.; Raghavachari, K.; Flood, A. H. *ChemPhysChem* **2009**, *10*, 2535−2540. (b) Ramabhadran, R. O.; Hua, Y.; Flood, A. H.; Raghavachari, K. *Chem.—Eur. J.* **2011**, *17*, 9123−9129.

(4) Selected literature for works in C−H hydrogen-bond donors: (a) Farnham, W. B.; Roe, D. C.; Dixon, D. A.; Calabrese, J. C.; Harlow, R. L. *J. Am. Chem. Soc.* **1990**, *112*, 7707−7718. (b) Desiraju, G. R.; Steiner, T. *The Weak Hydrogen Bond in Structural Chemistry and Biology*; Oxford University Press: New York, 1999. (c) Lee, C.-H.; Na, H.-K.; Yoon, D.-W.; Won, D.-H.; Cho, W.-S.; Lynch, V. M.; Shevchuk, S. V.; Sessler, J. L. *J. Am. Chem. Soc.* **2003**, *125*, 7301−7306. (d) Chmielewski, M. J.; Charon, M.; Jurczak, J. *Org. Lett.* **2004**, *6*, 3501−3504. (e) Kwon, J. Y.; Jang, Y. J.; Kim, S. K.; Lee, K. H.; Kim, J. S.; Yoon, J. *J. Org. Chem.* **2004**, *69*, 5155−5157. (f) Ilioudis, C. A.; Tocher, D. A.; Steed, J. W. *J. Am. Chem. Soc.* **2004**, *126*, 12395−12402. (g) Maeda, H.; Kusunose, Y. *Chem.—Eur. J.* **2005**, *11*, 5661−5666. (h) Bryantsev, V. S.; Hay, B. P. *Org. Lett.* **2005**, *7*, 5031−5034. (i) Bryantsev, V. S.; Hay, B. P. *J. Am. Chem. Soc.* **2005**, *127*, 8282−8283. (j) Maeda, H.; Haketa, Y.; Nakanishi, T. *J. Am. Chem. Soc.* **2007**, *129*, 13661−13674. (k) Fujimoto, C.; Kusunose, Y.; Maeda, H. *J. Org. Chem.* **2006**, *71*, 2389−2394. (l) Zhu, S. S.; Staats, H.; Brandhorst, K.; Grunenberg, J.; Gruppi, F.; Dalcanale, E.; Lutzen, A.; Rissanen, K.; Schalley, C. A. *Angew. Chem., Int. Ed.* **2008**, *47*, 788−792. (m) Yoon, D. W.; Gross, D. E.; Lynch, V. M.; Sessler, J. L.; Hay, B. P.; Lee, C. H. *Angew. Chem., Int. Ed.* **2008**, *47*, 5038−5042. (n) Berryman, O. B.; Sather, A. C.; Hay, B. P.; Meisner, J. S.; Johnson, D. W. *J. Am. Chem. Soc.* **2008**, *130*, 10895−10897. (o) Lee, S.; Chen, C.-H.; Flood, A. H.

*Nat. Chem.* **2013**, 5, 704−710. (p) Hua, Y.; Liu, Y.; Chen, C.-H.; Flood, A. H. *J. Am. Chem. Soc.* **2013**, 135, 14401−14412.

(5) (a) Frisch, M. J.; Del Bene, J. E.; Binkley, J. S.; Schaefer, H. F., III *J. Chem. Phys.* **1986**, 84, 2279−2289. (b) Emsley, J. *Chem. Soc. Rev.* **1980**, 9, 91−124.

(6) (a) Kang, S. O.; Powell, D.; Day, V. W.; Bowman-James, K. *Angew. Chem., Int. Ed.* **2006**, 45, 1921−1925. (b) Kang, S. O.; Day, V. W.; Bowman-James, K. *Inorg. Chem.* **2010**, 49, 8629−8636.

(7) Abraham, Y.; Salman, H.; Suwinska, K.; Eichen, Y. *Chem. Commun.* **2011**, 47, 6087−6089.

(8) Lehaire, M.-L.; Scopelliti, R.; Severin, K. *Inorg. Chem.* **2002**, 41, 5466−5474.

(9) Selected papers in using bifluoride as ligands: (a) Murphy, V. J.; Hascall, T.; Chen, J. Y.; Parkin, G. *J. Am. Chem. Soc.* **1996**, 118, 7428−7429. (b) Whittlesey, M. K.; Perutz, R. N.; Greener, B.; Moore, M. H. *Chem. Commun.* **1997**, 2, 187−188. (c) Roe, D. C.; Marshall, W. J.; Davidson, F.; Soper, P. D.; Grushin, V. V. *Organometallics* **2000**, 19, 4575−4582. (d) Jasim, N. A.; Perutz, R. N.; Foxon, S. P.; Walton, P. H. *J. Chem, Soc., Dalton Trans.* **2001**, 11, 1676−1685. (e) José, V.; Gil-Rubio, J.; Bautista, D.; Sironi, A.; Masciocchi, N. *Inorg. Chem.* **2004**, 43, 5665−5675. (f) Vergote, T.; Nahra, F.; Welle, A.; Luhmer, M.; Wouters, J.; Mager, N.; Riant, O.; Leyssens, T. *Chem.—Eur. J.* **2012**, 18, 793−798.

(10) Selected papers in using bifluoride as reagents: (a) Bosch, P.; Camps, F.; Chamorro, E.; Gasol, V.; Guerrero, A. *Tetrahedron Lett.* **1987**, 28, 4733−4736. (b) Sanghera, J. S.; Hart, P.; Sachon, M. G.; Ewing, K. J.; Aggarwal, I. *J. Am. Ceram. Soc.* **1990**, 73, 1339−1346. (c) Vedejs, E.; Chapman, R. W.; Fields, S. C.; Lin, S.; Schrimpf, M. R. *J. Org. Chem.* **1995**, 60, 3020−3027. (d) Molander, G. A.; Biolatto, B. *J. Org. Chem.* **2003**, 68, 4302−4314. (e) Hayashi, T.; Ueyama, K.; Tokunaga, N.; Yoshida, K. *J. Am. Chem. Soc.* **2003**, 125, 11508−11509. (f) Ooi, T.; Takada, S.; Doda, K.; Maruoka, K. *Angew. Chem., Int. Ed.* **2006**, 45, 7606−7608. (g) Vergote, T.; Nahra, F.; Peeters, D.; Riant, O.; Leyssens, T. *J. Oganomet. Chem.* **2013**, 730, 95−103.

(11) (a) Manson, J. L.; Conner, M. M.; Schlueter, J. A.; Lancaster, T.; Blundell, S. J.; Brooks, M. L.; Pratt, F. L.; Papageorgiou, T.; Bianchi, A. D; Wosnitzae, J.; Whangbo, M.-H. *Chem. Commun.* **2006**, 42, 4894−4896. (b) Manson, J. L.; Schlueter, J. A.; Funk, K. A.; Sutherland, H. I.; Twamley, B.; Lancaster, T.; Blundell, S. J.; Baker, P. J.; Pratt, F. L.; Singleton, J.; McDonald, R. D.; Goddard, P. A.; Sengupta, P.; Batista, C. D.; Ding, L.; Lee, C.; Whangbo, M.-H.; Franke, I.; Cox, S.; Baines, C.; Trial, D. *J. Am. Chem. Soc.* **2009**, 131, 6733−6747. (c) Manson, J. L.; Warter, M. L.; Schlueter, J. A.; Lancaster, T.; Steele, A. J.; Blundell, S. J.; Pratt, F. L.; Singleton, J.; McDonald, R. D.; Lee, C.; Whangbo, M.-H.; Plonczak, A. *Angew. Chem., Int. Ed.* **2011**, 50, 1573−1576. (d) Manson, J. L.; Lapidus, S. H.; Stephens, P. W.; Peterson, P. K.; Carreiro, K. E.; Southerland, H. A; Lancaster, T.; Blundell, S. J.; Steele, A. J.; Goddard, P. A.; Pratt, F. L.; Singleton, J.; Kohama, Y.; McDonald, R. D.; Del Sesto, R. E.; Smith, N. A.; Bendix, J.; Zvyagin, S. A.; Kang, J.; Lee, C.; Whangbo, M.-H.; Zapf, V. S.; Plonczak, A. *Inorg. Chem.* **2011**, 50, 5990−6009.

(12) (a) Carr, D. W.; Craighead, H. G. *J. Vac. Sci. Technol. B* **1997**, 15, 2760−2763. (b) Kim, J.-H.; Lim, D. H. Y.; Gye, M. *J. Vac. Sci. Technol. B* **1998**, 16, 558−560. (c) Doughty, C.; Knick, D. C.; Bailey, J. B.; Spencer, J. E. *J. Vac. Sci. Technol. A* **1999**, 17, 2612−2618.

(13) (a) Zhang, W.; Hu, Z.; Liu, Y.; Chen, H.; Gao, S.; Gaschnig, R. M. *Anal. Chem.* **2012**, 84, 10686−10693. (b) Kabangu, M. J.; Crouse, P. L. *Hydrometallurgy* **2012**, 129, 151−155.

(14) (a) Goldcamp, M. J.; Goldcamp, D. M.; Ashley, K.; Fernback, J. E.; Agrawal, A.; Millson, M.; Marlow, D.; Harrison, K. *J. Occup. Environ. Hyg.* **2009**, 6, 735−744. (b) Li, G.; Rao, M.; Li, Q.; Peng, Z.; Jiang, T. *Trans. Nonferrous Met. Soc. China* **2010**, 20, 1517−1520.

(15) Bhatti, Z. A.; Mahmood, Q.; Raja, I. A.; Malik, A. H.; Khan, M. S.; Wu, D. *Phys. Chem. Earth* **2011**, 36, 465−469.

(16) (a) Chuang, R.; Exelbert, E. J.; Heard, K. J. *Clin. Toxicol.* **2009**, 47, 741−741. (b) Maddry, J.; Brozovich, D.; Heard, K. *Clin. Toxicol.* **2012**, 50, 601−602. (c) Toledo, F.; Silvestre, J. F.; Cuesta, L.; Banuls, J. *Pediatr. Dermatol.* **2013**, 30, 145−147.

(17) Gormley, J. *Professional Carwashing and Detailing* **2001**, 25, issue 1.

(18) Bifluoride is the most important congenitor of fluoride. Its formation begins when basic fluoride anion abstracts a proton from an appropriate source to form HF, which is a competent Lewis acid. Subsequently, a strong hydrogen bond[5] is formed between the Lewis acidic HF and Lewis basic $F^-$ generating bifluoride, $HF_2^-$, as the adduct. The proton sources capable of driving this equilibrium are everywhere. First, solvents contain activated hydrogen atoms, e.g., chloroform and acetonitrile.[19] In these solvents, bifluoride formation will ideally be observed upon addition of fluoride and might even become the dominating fluoride-containing species when equilibrium is achieved.[6a] Second, trace amounts of water may be present. Third, fluoride salts, like the tetrabutylammonium fluoride that is commonly used in $F^-$ binding studies, normally contain finite waters of crystallization, and anhydrous forms of fluoride[20] are not straightforward to generate. Fourth, the hydrogen-bond donors present in anion receptors are also sources.[21] Consequently, the formation of bifluoride is commonly observed when more than 1.0 equiv of fluoride is added during a titration. In water, the stability of bifluoride is subject to equilibration[22] such that it is only present in acidic media and at higher concentrations. At a concentration above 10 mM, bifluoride is present from pH 1 to 6. Bifluoride will dissociate into fluoride in basic aqueous media, where the hydroxide ions dominate over hydronium ions. These alkali solutions and at low concentrations are probably the only exceptions where bifluoride is not present in the same solutions as fluoride. Other than these conditions, bifluoride is ubiquitous in the media where fluoride binding studies are conducted.

(19) Christe, K.; Wilson, W. W.; Wilson, R. D.; Bau, R.; Feng, J.-A. *J. Am. Chem. Soc.* **1990**, 2, 7619−7625.

(20) (a) Sun, H.; DiMagno, S. G. *J. Am. Chem. Soc.* **2005**, 127, 2050−2051. (b) Aragay, G.; Frontera, A.; Lloveras, V.; Vidal-Gancedo, J.; Ballester, P. *J. Am. Chem. Soc.* **2013**, 135, 2620−2627.

(21) (a) Boiocchi, M.; Del Boca, L.; Gomez, D. E.; Fabbrizzi, L.; Licchelli, M.; Monzani, E. *J. Am. Chem. Soc.* **2004**, 126, 16507−16514. (b) Gu, R.; Depraetere, S.; Kotek, J.; Budka, J.; Wagner-Wysiecka, E. W.; Biernat, J. F.; Dehaen, A. *Org. Biomol. Chem.* **2005**, 3, 2921−2923. (c) Evans, L. S.; Gale, P. A.; Light, M. E.; Quesada, R. *New J. Chem.* **2006**, 30, 1019−1025. (d) Cametti, M.; Rissanen, K. *Chem. Commun.* **2009**, 20, 2809−2829. (e) Juwarker, H.; Lenhardt, J. M.; Castillo, J. C.; Zhao, E.; Krishnamurthy, S.; Jamiolkowski, R. M.; Kim, K.-H.; Craig, S. L. *J. Org. Chem.* **2009**, 74, 8924−8934.

(22) Haque, R.; Reeves, L. W. *J. Am. Chem. Soc.* **1967**, 89, 250−252.

(23) Cametti, M.; Rissanen, K. *Chem. Soc. Rev.* **2013**, 42, 2016−2038.

(24) Selected reviews regarding fluoride binding and sensing: (a) Snowden, T. S.; Anslyn, E. V. *Curr. Opin. Chem. Biol.* **1999**, 3, 740−746. (b) Sessler, J. L.; Camiolo, S.; Gale, P. A. *Coord. Chem. Rev.* **2003**, 240, 17−55. (c) Gunnlaugsson, T.; Glynn, M.; Tocci, G. M.; Kruger, P. E.; Pfeffer, F. M. *Coord. Chem. Rev.* **2006**, 250, 3094−3117. (d) Cametti, M.; Rissanen, K. *Chem. Commun.* **2009**, 20, 2809−2829. (e) Wade, C. R.; Broomsgrove, A. E. J.; Aldridge, S.; Gabbai, F. P. *Chem. Rev.* **2010**, 110, 3958−3984.

(25) Hua, Y.; Ramabhadran, R. O.; Uduehi, E. O.; Karty, J. A.; Raghavachari, K.; Flood, A. H. *Chem.—Eur. J.* **2011**, 17, 312−321.

(26) McDonald, K. P.; Ramabhadran, R. O.; Lee, S.; Raghavachari, K.; Flood, A. H. *Org. Lett.* **2011**, 13, 6260−6263.

(27) Hay, B. P.; Firman, T. K. *Inorg. Chem.* **2002**, 41, 5502−5512.

(28) Hay, B. P. *Chem. Soc. Rev.* **2010**, 39, 3700−3708.

(29) (a) Hay, B. P.; Firman, T. K.; Lumetta, G. J.; Rapko, B. M.; Garza, P. A.; Sinkov, S. I.; Hutchison, J. E.; Parks, B. W.; Gilbertson, R. D.; Weakley, T. G. R. *J. Alloys Compd.* **2004**, 374, 416−419. (b) Hay, B. P.; Gutowski, M.; Dixon, D. A.; Garza, J.; Vargas, R.; Moyer, B. A. *J. Am. Chem. Soc.* **2004**, 126, 7925−7934. (c) Hay, B. P.; Firman, T. K.; Moyer, B. A. *J. Am. Chem. Soc.* **2005**, 127, 1810−1819. (d) Hay, B. P.; Oliferenko, A. A.; Uddin, J.; Zhang, C. G.; Firman, T. K. *J. Am. Chem. Soc.* **2005**, 127, 17043−17053. (e) Bryantsev, V. S.; Hay, B. P. *J. Am. Chem. Soc.* **2006**, 128, 2035−2042. (f) Bryantsev, V. S.; Hay, B. P. *J. Phys. Chem. A* **2006**, 110, 4678−4688. (g) Reyheller, C.; Hay, B. P.; Kubik, S. *New J. Chem.* **2007**, 31, 2095−2102. (h) Custelcean, R.;

Bosano, J.; Bonnesen, P. V.; Kertesz, V.; Hay, B. P. *Angew. Chem., Int. Ed.* **2009**, *48*, 4025−4029.

(30) Mascal, M.; Armstrong, A.; Bartberger, M. D. *J. Am. Chem. Soc.* **2002**, *124*, 6274−6276.

(31) (a) Mascal, M. *Angew. Chem., Int. Ed.* **2006**, *45*, 2890−2893. (b) Mascal, M.; Yakovlev, I.; Nikitin, E. B.; Fettinger, J. C. *Angew. Chem., Int. Ed.* **2007**, *46*, 8782−8784.

(32) (a) Houk, K. N.; Nakamura, K.; Sheu, C.; Keating, A. E. *Science* **1996**, *273*, 627−629. (b) Wang, X.; Houk, K. N. *Org. Lett.* **1999**, *1*, 591−594. (c) Helgeson, R.; Heyden, A. E.; Houk, K. N. *J. Org. Chem.* **2010**, *75*, 570−575. (d) Wang, H.; Liu, F.; Helgeson, R.; Houk, K. N. *Angew. Chem., Int. Ed.* **2012**, *52*, 655−659. (e) Edwards, N.; Helgeson, R.; Zhao, Y.; Houk, K. N. *Mol. Cryst. Liq. Cryst.* **2006**, *456*, 175−192.

(33) Frisch, M. J. et al. *Gaussian Development Version, Revision H.08*; Gaussian Inc.: Wallingford, CT, 2010.

(34) Zhao, Y.; Truhlar, D. G. *Theor. Chem. Acc.* **2008**, *120*, 215−241.

(35) Mayer, I.; Surjan, P. R. *Chem. Phys. Lett.* **1992**, *191*, 497−499.

(36) Huheey, J. E.; Keiter, E. A.; Keiter, R. L. *Inorganic Chemistry Principles of Structure and Reactivity*; Harper Collins: New York, 1993.

(37) (a) Morgan, G.; McKee, V.; Nelson, J. *J. Chem. Soc., Chem. Commun.* **1995**, *16*, 1649−1652. (b) Mason, S.; Llinares, J. M.; Morton, M.; Clifford, T.; Bowman-James, K. *J. Am. Chem. Soc.* **2000**, *122*, 1814−1815.

(38) The qualitative analysis performed in HySS to simulate the titrations under UV−vis concentrations shows that the 2:1 complex, $1_2 \cdot HF_2^-$, is present at low relative amounts (Figure S16, Supporting Information). Although there are three absorbing species, triazolophane **1**, the 1:1 complex $1 \cdot HF_2^-$, and a residual amount of the 2:1 complex $1_2 \cdot HF_2^-$, present during UV−vis titration as based on an unrestricted factor analysis of the data, the sandwich complex was present at such low amounts that including it did not result in reasonable fitting outcomes. Consequently, $1_2 \cdot HF_2^-$ was excluded from the data fitting.

(39) Vander Griend, D. A.; Bediako, D. K.; DeVries, M. J.; DeJong, N. A.; Heeringa, L. P. *Inorg. Chem.* **2008**, *47*, 656−662.

(40) The deformation energy measures the energy difference between the geometry of the macrocycle in its lowest energy conformation and after it has changed shape to accommodate the guest.

(41) The solubility of **2** is limited in $CH_2Cl_2$, which only allows for UV−vis titrations. On account of the fact that $CH_2Cl_2$ has similar solvent property as $CHCl_3$, the models established in NMR titrations are transferrable to UV−vis studies.